

# A Statistical Study of DORT Method for Locating Soft Faults in Complex Wire Networks

M. Kafal, J. Benoit, Andréa Cozza, Lionel Pichon

► **To cite this version:**

M. Kafal, J. Benoit, Andréa Cozza, Lionel Pichon. A Statistical Study of DORT Method for Locating Soft Faults in Complex Wire Networks. IEEE Transactions on Magnetics, Institute of Electrical and Electronics Engineers, 2018, 54 (3), pp.8700304. 10.1109/TMAG.2017.2765463 . hal-01639241

**HAL Id: hal-01639241**

**<https://hal-centralesupelec.archives-ouvertes.fr/hal-01639241>**

Submitted on 20 Nov 2017

**HAL** is a multi-disciplinary open access archive for the deposit and dissemination of scientific research documents, whether they are published or not. The documents may come from teaching and research institutions in France or abroad, or from public or private research centers.

L'archive ouverte pluridisciplinaire **HAL**, est destinée au dépôt et à la diffusion de documents scientifiques de niveau recherche, publiés ou non, émanant des établissements d'enseignement et de recherche français ou étrangers, des laboratoires publics ou privés.

# A Statistical Study of DORT Method for Locating Soft Faults in Complex Wire Networks

M. Kafal<sup>1</sup>, J. Benoit<sup>1</sup>, A. Cozza<sup>2</sup>, and L. Pichon<sup>2</sup>

<sup>1</sup>CEA, LIST, Laboratoire de Fiabilisation et d'Intégration des Capteurs Nano-Innov, 91191 Gif-sur-Yvette, France

<sup>2</sup>Group of Electrical Engineering - Paris, CentraleSupélec, Université Paris-Saclay, 91192 Gif-sur-Yvette, France

**Decomposition of the time-reversal (TR) operator (DORT), a recently applied TR method to transmission lines, has proven to be effective in detecting and locating soft faults in complex wire networks. In this paper, we will propose a fault location criterion which will form a later basis for a statistical study investigating the influence of several parameters, namely, the number of testing ports and the position of the fault, on the performance of DORT technique. Notably, this would allow a closer inspection of the method's practicability for future implementation in real-life networks.**

**Index Terms**—Complex wire networks, decomposition of the time-reversal (TR) operator (DORT) method, soft fault location, statistical study.

## I. INTRODUCTION

**E**LECTRICAL cables are in almost all modern systems where the transfer of energy and information is necessary to guarantee a proper functioning and a good performance of a system. Accordingly, safety issues related to faulty electrical wiring necessitated the availability of techniques capable of detecting the presence of faults that could potentially put in jeopardy a whole system. Several wire diagnosis methods have been introduced during the last few decades among which reflectometry techniques formed a spearhead [1], [2]. Conceptually based on analyzing fault reflected echoes, hard faults (open or short circuits) could be accurately located. On the other hand, the direct use of reflectometry techniques in networks, including junctions, e.g., Y-shaped networks, can properly detect the distance between the fault and the testing port, but cannot distinguish on what side the fault is located. Besides, the detection and location of soft faults, which are characterized by weak reflectivities, seemed to be critical [3].

Based on a radically different concepts, time-reversal (TR)-based methods originally developed in acoustics as remote sensing techniques [4] have shown to be effectual in locating soft faults in complex branched wire networks [5]–[8]. For instance, decomposition of the TR operator (DORT), a computational TR method, relies on the analysis of the network's TR operator (TRO) in an effort to synthesize customized testing signals. Notably, these signals are bound to focus over the fault position once injected into the ports of a network under test (NUT). In fact, the standard version of DORT (SDORT) as presented in [6] and the updated scheme (EDORT) in [7] proved to allow selective focusing and location of single as well as multiple soft faults in different complexity NUTs.

In particular, the process of locating a fault by DORT methods relied on localizing the energy peak associated with the constructive interference of the injected testing signals

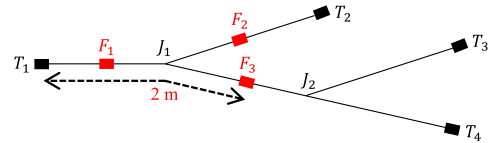


Fig. 1. Layout of a DJ NUT containing several soft faults on different positions.

on the fault position. Although, this allowed a clear identification when dealing with simple network structures and sufficient number of testing ports, an increasing complexity in interpretation was noticed when branched networks were addressed. Regrettably, the situation is expected to worsen when a deficiency in the number of testing ports occurs. Therefore, we will propose in this paper a contrast enhanced method for a more accurate localization of soft faults in branched networks. This will be followed by a statistical investigation studying the influence of the number of testing ports and the fault position on DORT's performance.

## II. FAULT LOCATION CRITERION USING THE DORT METHOD

As opposed to reflectometry techniques, DORT methods do not locate faults by monitoring the first significant reflected echo, but rather seek out the maximal fault-related focal region resulting from the propagation of focusing excitation signals across an NUT. Besides, the guided nature of transmission lines imposes that these signals also interact with each other and with junctions present in complex networks, therefore producing spurious constructive interferences at different positions of the network.

Unfortunately, the situation is even expected to worsen once the number of testing ports, consequently testing signals, decreases. To better illustrate this point, let us consider the double junction (DJ) NUT of Fig. 1 assuming the presence of a single soft fault  $F_3$  at a distance 2 m from reference port  $T_1$ . We considered two different testing-port configurations, the first comprises all four testing ports while only two are accounted in the second ( $T_1$  and  $T_3$ ). Notably, all remaining non-testing extremities are matched. After applying SDORT on both configurations, the energy is traced along

Manuscript received June 27, 2017; revised October 5, 2017; accepted October 11, 2017. Corresponding author: M. Kafal (e-mail: moussa.kafal@gmail.com).

Color versions of one or more of the figures in this paper are available online at <http://ieeexplore.ieee.org>.

Digital Object Identifier 10.1109/TMAG.2017.2765463

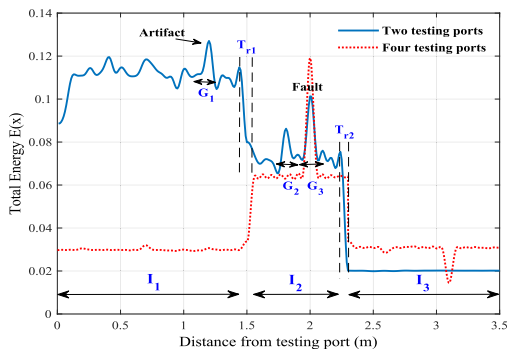


Fig. 2. Energy diagram of the DJ NUT of Fig. 1 after applying SDORT for four and two testing-port configurations observed along the third path.

the third path (linking  $T_1$  to  $T_3$ ) of the NUT, as demonstrated in Fig. 2. It can be clearly noticed that for the four testing-port configuration, testing signals have synchronized on the fault position which is characterized by a lucid focal region. On the other hand, as soon as we address the two testing-port configuration, the contrast between the total energy observed at the fault position and the background energy elsewhere deteriorates. In fact, ambiguity overwhelms the eventual fault location as spurious artifacts that appear as a result of junction-related signal interferences might be misinterpreted as fault positions.

In other words, if we consider the absolute values of the energy peaks, the dominant value will be that of the peak situated at 1.2 m from  $T_1$ , and not corresponding to the actual fault position. But, if we define  $I_i$ , the delimiting intervals, which represent different level transitions in the energy diagram, and we consider the amplitude of each peak relative to the local plateau ( $I_1$ ,  $I_2$ , or  $I_3$ ); the fault peak will be the dominant one and its detectability becomes direct and easy. Accordingly, considering the relative amplitudes of the peaks instead of the absolute ones shall solve this ambiguity.

As a result, a heuristic contrast-based fault location criterion is derived. In the first place, after defining the delimiting intervals  $I_i$ ,  $G_i$  intervals which are intervals contained in  $I_i$  are also defined. In fact, level transitions occur not only at the discontinuities positions, but also at different positions where echoes interfere. Consequently the points in the vicinity of these positions should not be accounted for when calculating the contrast. Therefore, the points contained in the intervals  $G_i$  will be excluded from the contrast calculation. To conclude, points having the same value of the plateau will belong to one of the intervals  $I_i$  but not to any of the intervals  $G_i$ .

It is worth to note that a Gaussian window ( $H(f) = e^{-f^2/(2\sigma^2)}/\sigma (2\pi)^{1/2}$ , with  $\sigma$  being a constant that controls the width of the Gaussian “bell”) has been applied to the testing signals before being injected into the NUT so as to reduce the secondary peaks. Consequently, this would facilitate the definition of the mean value of the plateau. To practically define  $G_i$ , we need to find a certain threshold, i.e., a fraction of the maximal amplitude of the Gaussian curve which we chose next to be  $1/10$ . This choice was based on the practical assumption that the amplitudes  $\leq 1/10$  of the maximal amplitude can be considered negligible, and thus, the corresponding points can be considered not to belong to any interval  $G_i$ . On the opposite, points whose amplitudes  $\geq 1/10$  of the maximal amplitude will be considered to belong to one of the intervals  $G_i$ , and consequently will be dropped when calculating the local plateau value. Let us now denote by  $\Delta_t$ ,

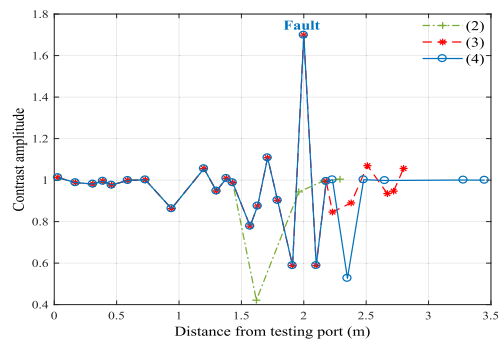


Fig. 3. Contrast computed along the different paths of the NUT of Fig. 1 for the two testing-port NUT configuration.

the time interval where the amplitude of the temporal Gaussian window decreases from its maximal value to  $1/10$  of this value, and by  $\Delta_f$  the frequency interval where the same attenuation affects the frequency Gaussian window (the Fourier transform of the temporal window), then a simple relation links the frequency support  $\Delta_f$  to  $\Delta_t$  as follows:

$$\Delta_t \Delta_f = \ln(10)/\pi$$

where we have

$$\Delta_f = \sigma \sqrt{2 \ln(10)}.$$

Consequently, by calculating  $\Delta_t$ , we can calculate the temporal width  $G_i$  as being equal to  $2\Delta_t$ . The same applies when calculating the limits of the intervals  $I_i$ ; here we excluded the points situated in the vicinity of the discontinuities, within a distance of  $\Delta_t/2$  from the discontinuity's position.

Having defined each of the delimiting intervals  $I_i$  and  $G_i$ , and calculated the plateau related to each one of them, we proceed to the calculation of the contrast of the local peaks. It is found by computing the ratio of the amplitude of the peak to that of the corresponding plateau previously calculated. Therefore, the highest contrast peak hints at the location of the fault.

For illustration purposes, we reconsidered the example of the two testing-port network configuration with a fault located at  $F_3$ , as shown in Fig. 1. The corresponding contrast diagram for all paths is presented in Fig. 3. The absence of focusing along path (2) shows that the fault is not located between  $T_1$  and  $T_2$ . Therefore, it shall be situated on the third or fourth path, at a distance 2 m from  $T_1$  that is on the branch linking the two junctions  $J_1$  and  $J_2$ . Accordingly, the proposed approach showed the ability to precisely locate the fault position in an NUT (distance from testing port, and position with respect to the branches).

It is worth to note that the whole process is typically executed in a matter of milliseconds using a standard state-of-the-art computer. On the other hand, alternative approaches related to reflectometry techniques that have been recently developed for the same purpose [2] can be very time consuming and their efficiency depends on the complexity of the network.

### III. STATISTICAL STUDY

The previous example showed that the performance of DORT is influenced by the number of testing ports and their positions. Apart from these two factors, the fault position is also expected to have an impact on whether to allow or not locate faults in an NUT. Thus, analyzing these parameters

and their possible effects on DORT's performance through a statistical study shall be of great interest.

### A. Database Definition

In order to conduct the statistical study, a database containing a large number of NUTs is necessary. The DJ NUT earlier studied serves as a good choice, as it is considered to be complex enough compared to those usually studied in this domain (single cables in most cases).

A total of four testing ports can be inserted on the extremities  $T_i$ , having  $i = 1, 2, \dots, 4$ . They were set matched ends in case they did not serve as testing ports. Three fault positions  $F_i$  ( $i = 1, 2, 3$ ) were considered where for each position, we generated a set of NUTs, whose branch lengths were randomly chosen. For each of these configurations, we also considered the cases of having 1, 2, 3, and 4 testing ports where we generated a total set of 4500 different files.

### B. Estimator of the Fault Location Probability

After establishing the statistical study's database, we designed several functions aiming to extract and analyze the desired information, based on the contrast location criterion earlier developed in Section II. The first step is to determine the contrast for all the peaks in the NUT followed by choosing the maximum contrast. If its spatial position corresponds to the fault one, we consider that the fault is located, if not, the fault is not correctly located. Consequently, this will provide the rates of the number of successes (i.e., when we locate the fault for a given NUT) to the total number of analyzed NUTs. This rate will be referred to as  $P_{sr}$ , with sr being the success rate. On the other hand, in order to have a better idea of the value of the location probability, we proceeded to an estimation of the latter based on the maximum likelihood estimation (MLE) whose probability is referred to as  $P_{MLE}$  with a corresponding 95% confidence interval (denoted as 95%  $c_i$ ) of  $P_{MLE}$ . Markedly, the MLE is a powerful estimator that allows obtaining a better estimation of the probability value than the frequency of occurrence does, given the relatively low number of analyzed NUTs.

### C. Influence of the Relative Position of the Fault

As we have mentioned earlier, the fault position is an important factor that is expected to influence DORT's performance, namely, its distance from the testing ports. Therefore, we expressed this parameter in terms of a ratio of the fault distance to the nearest testing port for  $F_1$  and  $F_2$ , and to the nearest junction for  $F_3$  (the ratio is expressed as a percentage). For instance, the ratio for fault  $F_3$  is the distance between  $J_1$  and  $F_3$ , to the distance between  $J_1$  and  $J_2$ . Accordingly, if  $F_1$  is situated at 50% from  $T_1$ , that means it is in the middle of  $T_1$  and  $J_1$ , and so on.

For each value of the distance percentage, we considered the cases of 1, 2, 3, and 4 testing ports, with all their possible configurations. By configuration we mean their position in the NUT: for example, one testing port can be placed at any  $T_i$ , while two testing ports can be for example placed at  $T_1$  and  $T_2$ , or  $T_3$  and  $T_4$ , and so on. Table I summarizes the number of possible configurations for each case.

The results of  $P_{sr}$  corresponding to the three fault positions ( $F_1$ ,  $F_2$ , and  $F_3$ ) are shown in Table II. Observing the values of the obtained success rates for the three faults, we clearly

TABLE I  
NUMBER OF ANALYZED CONFIGURATIONS FOR EACH FAULT

NUMBER OF TESTING PORTS	1	2	3	4
NUMBER OF CONFIGURATIONS	40	80	80	10

TABLE II  
SUCCESS RATES  $P_{sr}$

Number of testing ports	Relative distance percentage									
	10%		20%		40%		50%		70%	
1	0	0	0	0	0	0	0	0	0	0
2	0.52	0.74	0.52	0.74	0.52	0.74	0.52	0.74	0.52	0.74
3	0.75	1	0.75	1	0.75	1	0.75	1	0.75	1
4	1	1	1	1	1	1	1	1	1	1

$P_{sr}$  for the localization of faults  $\{F_1, F_2\}$  (in white), and  $\{F_3\}$  (in grey) in terms of the distance percentages relative to the extremities  $\{T_1, T_2\}$  and junction  $\{J_1\}$  respectively.

TABLE III  
ESTIMATED LOCATION PROBABILITY  $P_{MLE}$  AND 95%  $c_i$  FOR  $F_1$  AND  $F_2$

NUMBER OF TESTING PORTS	$P_{sr}$	$P_{MLE}$	95% $c_i$
1	0	0	[0; 0.0881]
2	0.52	0.5875	[0.4178; 0.6965]
3	0.75	0.8	[0.588; 0.8231]
4	1	1	[0.6306; 1]

TABLE IV  
ESTIMATED LOCATION PROBABILITY  $P_{MLE}$  AND 95%  $c_i$  FOR  $F_3$

NUMBER OF TESTING PORTS	$P_{sr}$	$P_{MLE}$	95% $c_i$
1	0	0	[0; 0.0881]
2	0.74	0.7645	[0.6464; 0.8263]
3	0.1	1	[0.9119; 1]
4	1	1	[0.6306; 1]

notice that they do not depend on the percentage of the fault distance from the corresponding extremity. Specifically, this validates that the distance parameter is not expected to influence the probability of localization, based on the fact that the DORT yields signals that focus on the fault position. In fact, propagation delays in terms of distances are directly compensated by the TRO definition. We can also realize that the faults  $F_1$  and  $F_2$  are equivalent in terms of probabilities; indeed, the two faults have equivalent positions when it comes to testing ports: they are both "seen" by a single testing port from one side, and by the others from the other side. Consequently, we will later reduce the number of studied faults to two,  $F_1$  and  $F_3$ .

Let us now estimate the probabilities  $P_{MLE}$  taking into account the previous observations. Thus, we consider the two faults  $F_1$  and  $F_3$ , and one set of success rates corresponding to a certain relative distance percentage (given that there is the same set of success rates for all the percentages). The case of fault  $F_1$  is shown in Table III, while the one corresponding to the second fault  $F_3$  is shown in Table IV. In the two cases, one testing port leads to a null location probability, whereas adding more testing ports increases this probability so as to reach 1 when using four testing ports. In the case of fault  $F_1$ , situated in front of the testing port  $T_1$ , i.e., not masked from this port by any junction or discontinuity, DORT fails in locating the fault when standard reflectometry methods succeed. Consequently, DORT methods do not present any advantage over reflectometry techniques in this particular case. Significantly, this was predicted when we considered the preliminary study in Section II, where it was revealed

that the DORT synthesizes signals that focalize on the fault position, requiring the existence of testing ports from both sides of the fault. Hence, a more detailed analysis taking into account the configuration of the testing port relative to the fault is going to be presented in Section III-D, aiming to generalize these ideas.

The case of four testing ports leads to an estimated location probability of 1 in the case of  $F_1$ , with a 95% confidence interval of plausible values for the probability ranging from 0.6306 to 1. This refers to the fact that, if a sample of analyzed files is taken repeatedly from the same analyzed population (all the analyzed files), and a confidence interval calculated for each sample, then 95% of the intervals will include the unknown parameter  $P_{MLE}$ . In this case the width of the interval is 0.3694, while for one testing port it is 0.0881, suggesting that for the case of four testing ports, more files should be analyzed if we want to reduce the interval width, which will eventually increase the precision on calculated probability value  $p_{MLE}$ .

In the case of  $F_3$ , for the same number of testing ports, we notice a bigger value of  $p_{MLE}$  compared to the case of  $F_1$ . This will be explained based on the testing ports configuration that is going to be addressed in the next section. In this case, an estimated probability of 1 is reached with three testing ports, which points the advantage of DORT methods in such cases where we are able to directly locate the fault without any need for iterations. Based on the conclusion of the apparent invariance of the location probability with the fault distance percentage, we will limit the remaining analysis to a single relative distance, considered to be 40%.

#### D. Influence of Sources' Configuration and Number

As observed in Section III-C, the position of the testing ports regarding the fault one influences the ability of DORT to localize the fault. The aim of this section is to investigate this issue through a more extended study including several configurations of the testing ports. One testing port can be placed on one of the four positions  $T_i$ , meaning  $C_4^1$  different possibilities, where  $C_4^1$  is the number of possible combinations, when picking out one position in four potential choices ( $C_n^k$  being the binomial coefficient). In the same way, two testing ports can be chosen according to  $C_4^2$  different combinations, and so on. The total number of possible configurations of the testing ports is thus  $C_4^1 + C_4^2 + C_4^3 + C_4^4 = 15$ .

Based on all the possible configurations, we calculated the success rates when trying to locate the fault for the three positions  $F_1$ ,  $F_2$ , and  $F_3$  for each configuration. In particular, the results obtained in Table V show that one testing port leads to a null location probability which applies for the three fault locations. The testing signals synthesized using DORT are bound to focus on the fault position, and this focalization is hard to obtain if there are not testing ports from both sides of the fault.

TABLE V  
ESTIMATED LOCATION PROBABILITY  $P_{MLE}$

FAULT	NUMBER OF TESTING PORTS			
	1	2	3	4
$F_1$	0	0.5138	0.754	1
$F_3$	0	0.7183	1	1

Consequently, adding more testing ports increases the location probability which reaches 1 when all of four testing ports are used. Thus, based on the DORT properties and the preliminary analysis obtained, one can expect to have a higher location probability when testing ports exist from both sides of the fault (as that of  $F_3$ ), and a low location probability in the opposite cases.

#### IV. CONCLUSION

In this paper, a part of the elements influencing the performance of DORT method was investigated through a statistical study. It was revealed that the number and positions of network's testing ports played an important role in determining method's ability to locate a certain fault. It is necessary to have testing ports from both sides of the fault for a possible location of the fault.

In this event, it would also be greatly interesting to conduct a more extended study; starting with a wider database, including more network configurations, as well as an extension of the influencing parameters to include the bandwidth, losses, noise, and model perturbations.

#### REFERENCES

- [1] C. Furse, Y. C. Chung, C. Lo, and P. Pendayala, "A critical comparison of reflectometry methods for location of wiring faults," *Smart Struct. Syst.*, vol. 2, no. 1, pp. 25–46, 2006.
- [2] M. K. Smail, L. Pichon, M. Olivas, F. Auzanneau, and M. Lambert, "Detection of defects in wiring networks using time domain reflectometry," *IEEE Trans. Magn.*, vol. 46, no. 8, pp. 2998–3001, Aug. 2010.
- [3] M. K. Smail, T. Hacib, L. Pichon, and F. Loete, "Detection and location of defects in wiring networks using time-domain reflectometry and neural networks," *IEEE Trans. Magn.*, vol. 47, no. 5, pp. 1502–1505, May 2011.
- [4] C. Prada and M. Fink, "Eigenmodes of the time reversal operator: A solution to selective focusing in multiple-target media," *Wave Motion*, vol. 20, no. 2, pp. 151–163, Sep. 1994.
- [5] M. Kafal, J. Benoit, A. Cozza, and L. Pichon, "Soft fault diagnosis in wire networks using time reversal concept and subspace methods," in *Proc. EETEM*, to be published.
- [6] L. Abboud, A. Cozza, and L. Pichon, "A noniterative method for locating soft faults in complex wire networks," *IEEE Trans. Veh. Technol.*, vol. 62, no. 3, pp. 1010–1019, Mar. 2013.
- [7] M. Kafal, A. Cozza, and L. Pichon, "Locating multiple soft faults in wire networks using an alternative DORT implementation," *IEEE Trans. Instrum. Meas.*, vol. 65, no. 2, pp. 399–406, Feb. 2016.
- [8] M. Kafal, A. Cozza, and L. Pichon, "Locating faults with high resolution using single-frequency TR-MUSIC processing," *IEEE Trans. Instrum. Meas.*, vol. 65, no. 10, pp. 2342–2348, Oct. 2016.